Journal of Anatomy

Received: 7 October 2019 | Revised: 20 December 2019 | Accepted: 13 January 2020

DOI: 10.1111/joa.13161

ORIGINAL ARTICLE

ANATOMICAL SOCIETY Journal of Anatomy WILEY

Biomechanical properties of anuran long bones: correlations with locomotor modes and habitat use

Miriam Corina Vera[1] | José Luis Ferretti[2] | Virginia Abdala[3,4] | Gustavo Roberto Cointry[2]

[1]Laboratorio de Genética Evolutiva, Instituto de Biología Subtropical, Universidad Nacional de Misiones-CONICET, Misiones, Argentina

[2]Centro de Estudios de Metabolismo Fosfocálcico, Facultad de Ciencias Médicas, Universidad Nacional de Rosario-CONICET, Santa Fe, Argentina

[3]Cátedra de Biología General, Facultad de Ciencias Naturales e IML, Universidad Nacional de Tucumán, Tucumán, Argentina

[4]Instituto de Biodiversidad Neotropical, Universidad Nacional de Tucumán-CONICET, Tucumán, Argentina

Correspondence
Gustavo Roberto Cointry, Centro de Estudios de Metabolismo Fosfocálcico, Facultad de Ciencias Médicas, Universidad Nacional de Rosario-CONICET, Santa Fe, Argentina.
Email: gcointry@gmail.com

Funding information
Fondo para la Investigación Científica y Tecnológica, Grant/Award Number: PICT 2016-2772 ; Consejo Nacional de Investigaciones Científicas y Técnicas, Grant/Award Number: PIP 0389

Abstract

Long bones are subjected to mechanical loads during locomotion that will influence their biomechanical properties through a feedback mechanism (the bone mechanostat). This mechanism adapts the spatial distribution of the mineralized tissue to resist compression, bending and torsion. Among vertebrates, anurans represent an excellent group to study long bone properties because they vary widely in locomotor modes and habitat use, which enforce different skeletal loadings. In this study, we hypothesized that (a) the cortical bone mass, density and design of anuran femur and tibiofibula would reflect the mechanical influences of the different locomotor modes and habitat use, and (b) the relationships between the architectural efficiency of cortical design (cross-sectional moments of inertia) and the intrinsic stiffness of cortical tissue [cortical mineral density; the 'distribution/quality' (d/q) relationship] would describe some inter-specific differences in the efficiency of the bone mechanostat to improve bone design under different mechanical loads. To test this hypothesis, we determined tomographic (peripheral quantitative computed tomography) indicators of bone mass, mineralization, and design along the femur and tibiofibula of four anuran species with different modes of locomotion and use of habitat. We found inter-specific differences in all measures between the distal and proximal ends and mid-diaphysis of the bones. In general, terrestrial-hopper species had the highest values. Arboreal-walker species had the lowest values for all variables except for cortical bone mineral density, which was lowest in aquatic-swimmer species. The d/q relationships showed similar responses of bone modeling as a function of cortical stiffness for aquatic and arboreal species, whereas terrestrial-hoppers had higher values for moments of inertia regardless of the tissue compliance to be deformed. These results provide new evidence regarding the significant role of movement and habitat use in addition to the biomechanical properties of long bones within a morpho-functional and comparative context in anuran species.

KEYWORDS
anuran locomotion, bone biomechanics, bone mechanostat, femur, pQCT, tibia-fibula

1 | INTRODUCTION

In comparative biology, there is an increasing interest in analysing the influences of the mechanical environment on several aspects of tetrapod life, especially with regard to locomotion (Losos 1990a,1990b,1990c; Losos et al. 1991; Bauwens et al. 1995; Cruz et al. 2009; Tulli et al. 2011; Griep et al. 2013; Herrel et al. 2014; Cox and Gillis, 2015; Soliz et al. 2017; Fratani et al. 2018; Vera et al. 2018). Unusual locomotor demands on the limb skeleton, such as anuran jumping, are probably the most likely to show what kind of bone mechanical properties are more relevant to meet those demands (Blob and Snelgrove, 2006; Wilson et al. 2009).

Bones are subjected to daily mechanical loads, which are determined by gravitational forces and contractions of the associated muscles (Carter et al. 1998; Ferretti et al. 2001; Vizcaíno et al. 2016). In long bones, a feedback mechanism, the bone mechanostat (Frost, 2002), adapts the spatial distribution of the mineralized tissue to resist bending and torsion. This occurs through a directional modulation of bone modeling as a function of the magnitude and orientation of the strains induced by customary usage of the bones (Frost, 2002). During locomotion, the local deformations produced by the mechanical environment stimulate bone cells and orient bone adaptation (Frost, 1998; Hamrick et al. 2006). Both the directionality and intensity of the stimuli may vary for different bone regions (Hamrick et al. 2006; Cointry et al. 2016). Thus, the mechanical loads have a regional influence on mineral tissue mass and distribution (Kontulainen et al. 2008; Feldman et al. 2012), which usually determine bone structural stiffness, a factor in preventing fracture in mobile bones as a function of their customary mechanical usage in all vertebrates [the 'Utah Paradigm' (Frost, 2002)].

In general terms, the bone mechanostat proceeds within the geometric limits imposed by the phylogenetically determined morphogenesis of all vertebrate skeletons. Thus, in all vertebrates, the architectural design of all mobile bones depends on both morphogenetic and mechanical factors. Bone mechanical properties can be assessed by peripheral quantitative computed tomography (pQCT). This technology provides cortical indicators of: tissue mass [cortical bone area (CtA) and bone mineral content (BMC)]; tissue mineralization [cortical volumetric bone mineral density (vBMD)]; shell design (moments of inertia of the cross-section); and structural stiffness [bone strength indices [BSIs]; Ferretti et al. 1996). In addition, pQCT enables the efficiency of the biomechanical control of bone design to be evaluated at every site studied (i.e. efficiency of the bone mechanostat). In fact, the architectural efficiency of the bone mechanostat [orientation of 'modeling drifts' (Frost, 1990)] was shown to be inversely related to tissue stiffness (Ferretti, 1995; Ferretti et al. 1995; Di Masso et al. 1997; Feldman et al. 2004; Cointry et al. 2005, 2013, 2016). Thus, this relationship can be described by typical, negative curves obtained by correlating pQCT indicators of bone design related to cortical bone tissue 'distribution' (i.e. moments of inertia related to bending or torsion) and of bone tissue 'quality' (i.e. cortical vBMD). The corresponding graphs, known as 'distribution/quality' (d/q) curves (Ferretti, 1995; Ferretti et al. 1995; Di Masso et al. 1997; Feldman et al. 2004; Cointry et al. 2005, 2013, 2016), show that the higher the tissue compliance to deformation, the greater the moment of inertia value achieved by the system to improve the local resistance to natural bone strains. In d/q relationship graphs, a shift of the experimental data to the lower-left with respect to a reference curve suggests a 'catabolic' interaction with the bone mechanostat 'set point' (a reference strain for the system). Conversely, a shift to the upper-right side indicates an 'anabolic' interaction (Feldman et al. 2004). d/q curves have been used to describe the effects of gender, genetic factors, physical activity, bone-weakening diseases and different treatments on the bone mechanostat (Ferretti et al. 1995; Di Masso et al. 1997; Feldman et al. 2004; Cointry et al. 2005, 2013, 2016; Wang et al. 2009; Guilluy et al. 2014; Iskratsch et al. 2014; Tondon and Kaunas, 2014; Rolfe et al. 2014; Nadell and Shaw, 2015; Humphries et al. 2017), and may differ between species (Ferretti, 1995). This difference could reflect either or both the influence of their anatomical differences and the mechanical environments of their skeletons.

Several animal and clinical studies have shown that some structural variables can reflect the mechanical usage the bones are undergoing (Wilson et al. 2009). In connection with these studies, it was shown that the intensity, frequency and duration of each activity are first-order determinants of the effects of the mechanical environment on the skeleton (Morseth et al. 2011). Also, it was reported that the stimuli induced by jumping and other high-impact activities are more effective in optimizing the design of some bones through a directional modulation of bone modeling than those induced by running, walking and swimming (Morseth et al. 2011; Weidauer et al. 2014; Gomez-Bruton et al. 2015). This was revealed by increments in CtA, volumetric mineral density, thickness, and cross-sectional moments of inertia (Morseth et al. 2011; Weidauer et al. 2014; Gomez-Bruton et al. 2015). However, cortical vBMD is lower in swimmers than in terrestrial species and in human swimmers than in other trained individuals (Bourrin et al. 1992; Bellew and Gehrig, 2006; Mudd et al. 2007).

Amphibian anurans have a great variety of both locomotor modes (e.g. swimming, jumping, hopping, walking) and habitat use [e.g. terrestrial, aquatic, arboreal (Duellman and Trueb, 1986; Manzano et al. 2017; Soliz et al. 2017; Fratani et al. 2018)]. These very contrasting biological and ecological conditions will enforce different mechanical loading on the skeleton, mainly owing to differences in viscosity, density and gravitational force. In the aquatic medium, buoyancy plays a significant role in the determination of bone loads (Zug, 1971). By contrast, in terrestrial locomotion, gravity and ground reaction forces must be considered (Nauwelaerts and Aerts, 2003). The arboreal habitat is a complex environment that requires different mechanical properties, such as the modulation of the take-off force over an elastic substrate (Reynaga et al. 2019). Thus, locomotion in aerial habitats will demand higher muscle forces than in an aquatic medium (Biewener and Gillis, 1999). For all those reasons, we think that anurans would provide excellent models to study both bone mechanical properties and the mechanostat system. In this regard, serial pQCT studies of anuran whole long bones should provide the necessary data to assess the degree of mechanical adaptation of bone structure to a typical mechanical environment and detect any site-specific behavior of the mechanostat.

In the present study, we hypothesize that, in anurans, (a) the femur and tibiofibula would reflect the mechanical influences of the different locomotor modes and use of habitat, showing significant differences in bone mass, mineralization, design, or structural stiffness concerning the higher (jumping/hopping) or lower impact (swimming/walking) of their usual mechanical stimuli and (b) the relationships between the architectural efficiency of cortical design (cross-sectional moments of inertia) and the intrinsic stiffness of cortical tissue (cortical mineral density; d/q relationships) would describe some inter-specific differences in the efficiency of the bone mechanostat to improve bone design under different mechanical loads. To test these hypotheses, we determined specific structural properties of the femur and tibiofibula of four anuran species with very different locomotor modes, as assessed by pQCT. The bones selected for study have been typically shown to be sensitive to usage-dependent modeling/remodeling directional modulation in vertebrates (Hudson et al. 2004) and therefore are ideal for testing the relationships between bone structural variables and ecological aspects of locomotion in the species studied.

TABLE 1 Collection numbers and mean snout-vent lengths, femur lengths and tibiofibula lengths of the specimens studied.

Species (collection numbers)	SVL, mm	FL, mm	TFL, mm
Rhinella diptycha (LGE 3943, 7207, 18171, 18179, 18188, 18242)	136.89 ± 8.58	48.94 ± 3.52	47.61 ± 3.63
Boana faber (LGE 236, 268, 271, 1610, 17058)	91.35 ± 3.82	46.23 ± 1.4	50.73 ± 3.29
Phyllomedusa sauvagii (LGE 20719, 20721, 20722, 20724, 20725)	69.98 ± 2.36	27.37 ± 0.62	28.17 ± 0.73
Pseudis platensis (LGE 3999, 4001, 16745, 16758, 16761)	50.20 ± 3.02	26.58 ± 3.5	25.31 ± 3.22

LGE, *Laboratorio de Genética Evolutiva*; SVL, snout-vent length (SVL), FL, femur length TFL, tibiofibula length.

2 | MATERIAL AND METHODS

2.1 | Specimens

Twenty-two alcohol-preserved male adult specimens of four anuran species were selected for this study. The analysed specimens were from the Herpetological Collection of the *Laboratorio de Genética Evolutiva* (*Instituto de Biología Subtropical*); the collection numbers of the specimens are detailed in Table 1. Left hindlimbs were removed from the body, and muscle dissection was performed to isolate and analyze the femur and the tibiofibula. The species were selected according to their habitat use and locomotor modes: terrestrial-hopper (Te-H; *Rhinella diptycha*, n = 6), arboreal-jumper (Ar-J; *Boana faber*, n = 6), arboreal-walker (Ar-W; *Phyllomedusa sauvagii*, n = 5), and aquatic-swimmer species (Aq-S; *Pseudis platensis*, n = 5). These species represent two different anuran families, Bufonidae and Hylidae. Moreover, each species is representative of one specific use of habitat and locomotion mode that imposes differing functional demands.

2.2 | Peripheral quantitative computed tomography measurements

The entire femur and tibiofibula of each specimen were scanned with a pQCT scanner (XCT-2000; Stratec), software version 5.0. The slices were 2.5-mm thick. The in-plane pixel size was set at 0.1 mm, as allowed by the Stratec software for small animal studies. The scans of each bone were serially performed throughout at every 5% of the total bone length, starting at 5% of the bone length from the distal end and up to 90%, next to the proximal epiphysis. The scans were numbered from s5 (5% site; distal end of the bone) to s90 (90% site; proximal end of the bone); thus, a total of 18 scans were obtained per bone. As the results at s5 were less clear, we plotted bone parameters from s10.

Threshold values for total and cortical bone were selected at 710.0 mg/cm^3, using the parameters contmode 3, cortmode 3, and peelmode 3 for the femur and 2 for the tibiofibula. For inter-specific comparison, some variables were adjusted according to indicators of body size, such as CtA [an indicator of the uniaxial loading of the bone in compression derived from body mass bearing (Ferretti, 1998)] and bone length (Ruff, 2000) to eliminate the size effect (snout-vent length and bone length are detailed in Table 1). The following bone indicators from each scan were studied:

1. Bone mass indicators
    - Cortical BMC, defined as the mass of mineral per unit of bone scan thickness (mg/cm; Schoenau, 2005).
    - CtA, regarded as relevant to bone structural stiffness/strength in uniaxial compression (mm^2; Ferretti et al. 2001).
2. Bone tissue quality indicator
    - Cortical vBMD (mg/cm^3), the volumetric mineral density of the cortical tissue, regarded as indicative of bone tissue stiffness (Currey, 1999). To minimize measurement errors caused by the 'partial volume effect', cortical vBMD was corrected according to the equation proposed by Rittweger *et al.* (2004).

3. Bone design indicator (geometric bone properties)
   - Second moments of inertia of the cross-sectional cortical area (CSMIs). These indicators express the architectural efficiency of the cross-sectional design of the cortical shell (bone tissue 'distribution') to resist anterior-posterior (*x*CSMI) or lateral bending (*y*CSMI; Cointry et al. 2014). The CSMIs are the integral sums of the products between the area of each pixel of CtA in the image and its squared distance to the corresponding bending axis. All CSMI values were adjusted by the product of the CtA and the squared bone length (CSMI/[CtA*bone length^2]) to eliminate the size effect (Ruff, 2000).
4. Structural stiffness/strength indicators
   - Bone strength indices (*x*BSI = cortical vBMD × *x*CSMI, or *y*BSI = cortical vBMD × *y*CSMI): indicators of whole-bone quality; estimates of bone structural stiffness (a close correlate of whole-bone strength) in anterior-posterior or lateral bending (*x*BSI, *y*BSI, mg × mm), respectively. These indicators were adjusted by bone length (Ruff, 2000).
5. Distribution/quality relationships.
   - Correlations between the 'cross-sectional design indicators' (*x*CSMI or *y*CSMI, concerning anterior-posterior or lateral bending, *y*-axes) and the 'bone tissue stiffness indicators' (cortical vBMD, *x*-axes) values at each skeletal site from s50 to s80 were calculated as d/q relationships (Ferretti, 1995). The d/q relationships were regarded as indicators of the efficiency of the biomechanical control of the cortical shell design by the bone mechanostat.

2.3 | Statistical analyses

Differences between species were evaluated by one-way ANOVA after logarithmic transformation to normalize the data. Specific pairwise differences were identified with a *post-hoc* Tukey test. Differences were considered significant at $P < 0.05$. Simple correlation analyses were performed to evaluate the d/q relationships, and ANCOVA tests were used to assess the differences between intercepts and slopes of the d/q curves for different species data. The software STATISTICA (Statsoft) and the interface R studio (version 1.1.383) of the software R was used for these analyses.

3 | RESULTS

The size and shape of the femur and tibiofibula cross-sections (Figure 1) varied from site to site throughout the bones in the analyzed species. In the femurs, three general shapes were observed (Figure 1a): a rounded shape, present at proximal sections (s80) of all species and at s50–s20 in arboreal and aquatic species; a drop shape, formed by the presence of a femoral crest in s70–s50 in *R. diptycha* (Te-H), s70 in *B. faber* (Ar-J) and s70–s60 in *P. sauvagii* (Ar-W); and an elliptic shape at the distal section (s20), next to the knee joint in Te-H species. In the tibiofibula, three different general shapes could also be observed (Figure 1b): an elliptic-crown shape with an anterior-posterior band formed by the fusion of the tibia and the fibula which was visible at the proximal and distal sections (s80 and s20) in all the species except Ar-W and also at s70 and s30 in Te-H species; an elliptic-crown shape without the fusion band, as shown at s60 and s40 in Te-H and at s70 and s30 in Ar-J and aquatic species and at s70 and s20 in Ar-W; and a grossly rounded shape at mid-diaphysis (s60–s40) in Ar-J and aquatic species.

3.1 | Bone mass indicators

In general terms, in both femurs and tibiofibula, cortical BMC (Figure 2a,b) was higher in *R. diptycha* (Te-H) throughout the bones ($P < 0.001$) and, particularly in the femur, with higher values distally than proximally. *B. faber* (Ar-J) showed intermediate BMC values and significant differences ($P < 0.001$) from the rest of the species. *P. sauvagii* (Ar-W) and *Ps. platensis* (Aq-S) showed slightly lower BMC values than those of Ar-J. Within a short distal segment of the femurs (s10–s20), Ar-J and Aq-S showed similar BMC values, significantly higher than those shown by Ar-W species. In the tibiofibula (Figure 2b), Te-H showed higher values at both ends and the midshaft than at the central regions of the proximal and distal halves of the bone. Ar-J species had the highest BMC values at mid diaphysis and at the proximal end. In Ar-W and Aq-S species, there were similar BMC values along the bone, with a slight increase toward the distal region. Within the s10–s20 segment, these species showed similar and significantly lower values than Ar-J.

In the four species, the femur CtA values (Figure 2c) ranked grossly similarly to BMC values in all bone sites. The highest CtA values were reached toward the distal ends of both the femur and tibiofibula. Distally in the femur (s15), the CtA in Aq-S and Ar-J were similar and different from Ar-W. While at s35, s45 and s55–s75, aquatic and arboreal species showed similar values. At S50, Ar-J differed from Aq-S and Ar-W species ($P < 0.001$). The Ar-W species showed the lowest CtA values through the bone, except at s85, where arboreal and aquatic species presented similar values. These trends were comparable to those observed for the tibiofibula (Figure 2d).

3.2 | Bone tissue quality indicator

In the femurs, the cortical vBMD (Figure 3a) showed similar values between species at distal and proximal ends. It increased from s10 upwards, showing different patterns up to a maximum at s50–s60 in all the species and decreased proximally. Cortical vBMD was higher in Te-H at the distal half (s5–s50), while Ar-J showed the highest values at the proximal half (s50–s90). Aq-S species showed the lowest cortical vBMD values, and intermediate values were observed for Ar-W species (Figure 3b). Similar trends were observed in the tibiofibula except that Te-H and Ar-J species showed similar and higher

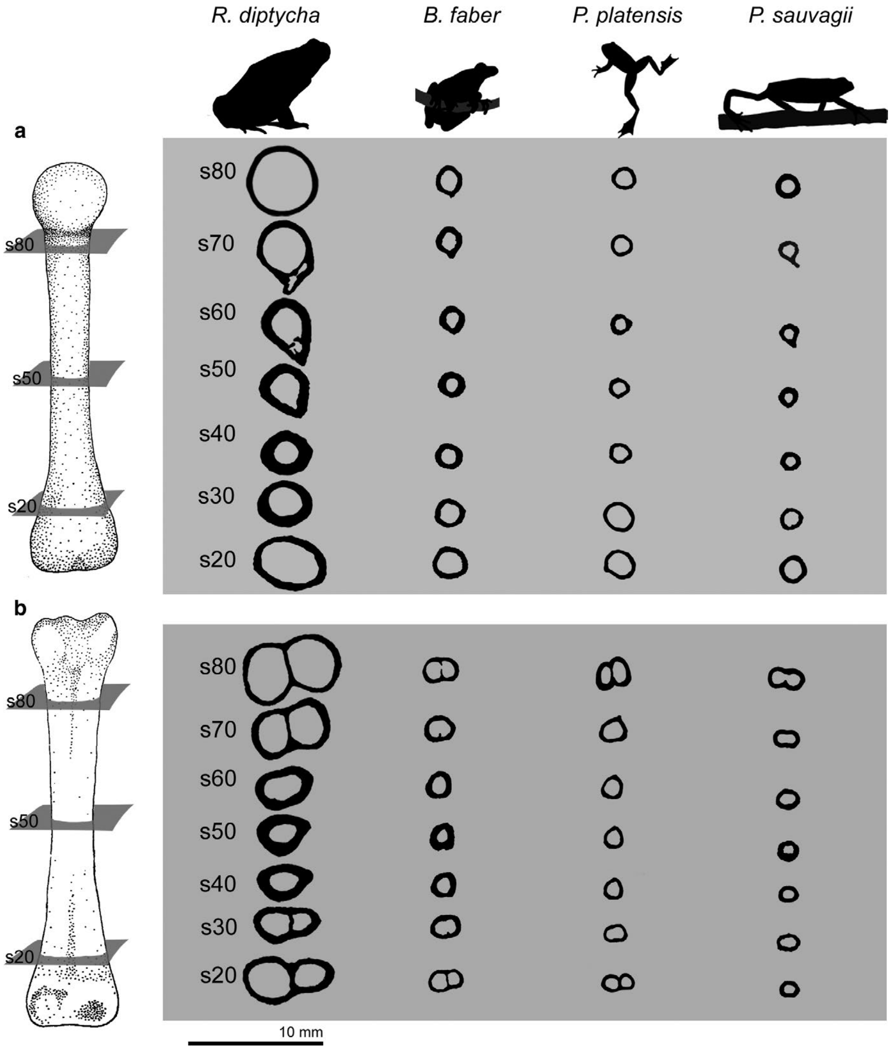

FIGURE 1 Some of the scans obtained from the studied sites of the different species analyzed. (a) Femur scans, (b) tibiofibula scans. Scale bar 10 mm.

values throughout the bone ($P < 0.001$). The lowest cortical vBMD values were observed in Ar-W and Aq-S species.

3.3 | Bone design indicators (geometric bone properties)

In the femurs of all analyzed species, the CSMI values were generally higher distally and proximally than at the mid-diaphyses (Figure 4a). The Te-H species showed the highest CSMI values in all femoral sites (Figure 4a). Central-distally (s10–s20), the CSMIs were intermediate for aquatic species, and the lowest for arboreal species (jumpers and walkers). Significant inter-group differences ($P < 0.001$) were observed, with some site-specificity. In Te-H species, and less noticeably in Ar-W species, the femur showed a crest on the posterior aspect (between s45 and s75), which determined an increment of the *x*CSMI values (Figure 4A). Also in Ar-W species, the *x*CSMI values increased significantly in s70–s90 to match the Aq-S values (Figure 4a). The tibiofibula showed a similar pattern to the femur, with lower CSMI values (Figure 4b). In this bone, the *x*CSMI was similar in Te-H and Aq-S species at s30–s65 (Figure 4b), while the *y*CSMI values were similar in the two arboreal species at those sections (Figure 4d). As observed in the femur, the CSMIs were significantly larger in Ar-W than in Ar-J species at proximal ends (s75–s85).

3.4 | Structural stiffness/strength indicators

In both femurs and tibiofibula, *x*BSI and *y*BSI were much higher in Te-H than in the other species, with similar values for Ar-J and Aq-S and lowest values for Ar-W species ($P < 0.001$). In the femur at s15–s50, Ar-J and Aq-S species showed similar BSI values, both significantly higher than those of Ar-W ($P < 0.001$; Figure 5a). In the tibiofibula, the BSI values of these two species were similar along the bone (Figure 5b).

3.5 | Distribution/quality relationships

The relationships observed between either of the CSMIs and the cortical vBMD of all the specimens studied between s50 and S80

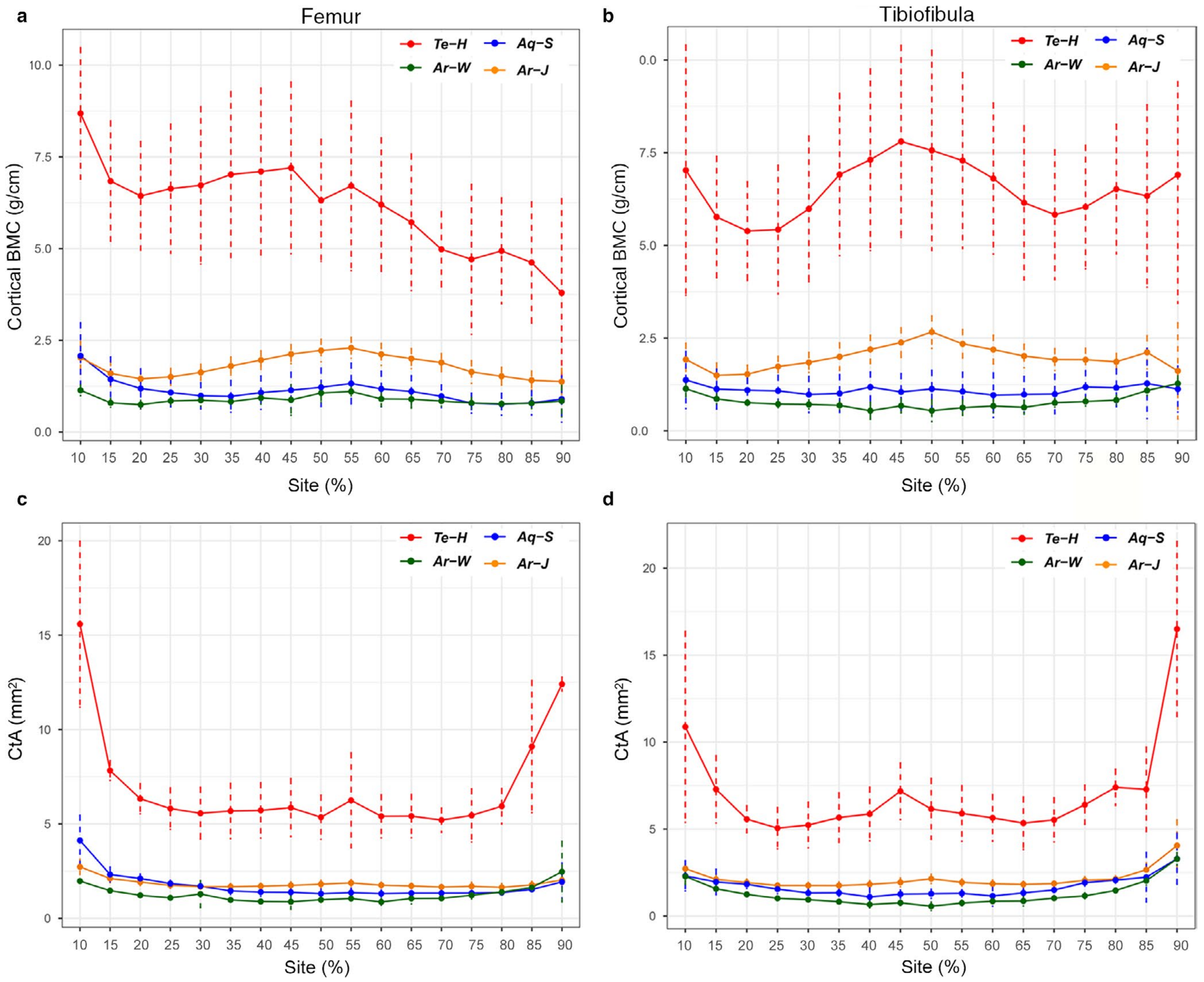

FIGURE 2 Bone mass indicators: cortical bone mineral content (BMC) of the femur (a), and the tibiofibula (b). Cortical bone area (CtA) of the femur (c), and the tibiofibula (d). Aq-S, aquatic swimmers; Ar-J, arboreal jumpers; Ar-W, arboreal walkers; Te-H, terrestrial-hoppers.

were described by negative, simil-hyperbolic correlation curves, which were best adjusted by negative exponential functions of the form y = a × exp(−b × x). *R. diptycha* (Te-H) curves shifted significantly to the upper-right zone with respect to the other species, showing a negative but not significant slope. In the other species the curves followed similar patterns for the femur (Figure 6a,c) and tibiofibula (Figure 6b,d). *Ps. platensis* (Aq-S) and *P. sauvagii* (Ar-W) data were plotted in the upper-left zone and those of *B. faber* (Ar-J) were plotted in the lower-right zone in all graphs.

4 | DISCUSSION

The femur cross-sections showed generally rounded shapes, especially at the mid-diaphysis of the arboreal and aquatic species and at s40 in terrestrial ones, suggesting an adaptation to torsion (Broshko, 2014) or multidirectional bending which are typical of arboreal locomotion (Demes and Carlson, 2009). On the other side, an elliptic shape with larger medial-lateral than anterior-posterior axes, suggesting resistance to lateral bending (Cointry et al. 2016), was shown at s30–s40 in the femur and throughout the tibiofibula in Te-H species and at s20–s30 and s70–s80 in the tibiofibula in all the other species. The 'drop shape' conferred to the proximal sections by the femoral crest (which sharply increases the xCSMI) in Te-H, and less noticeably in Ar-W species, indicates a higher resistance to anterior-posterior bending (Broshko, 2014), as required by the loading of the bones during locomotion in a terrestrial environment (Demes and Carlson, 2009; Cointry et al. 2014).

Our data tend to support our first hypothesis; in fact, we recorded significant differences in bone indicators among locomotor modes and habitat use. The Te-H species (*R. diptycha*) showed the highest values for almost all the allometrically related variables, especially at both femoral ends. The cortical bone mass variables (BMC and CtA) indicated a difference in bone size between this and the other three species. Curiously, in the femur of Te-H species, the BMC values decreased proximally despite the increase in CtA. In the tibiofibula, the distribution of the cortical BMC values was similar for all species, with

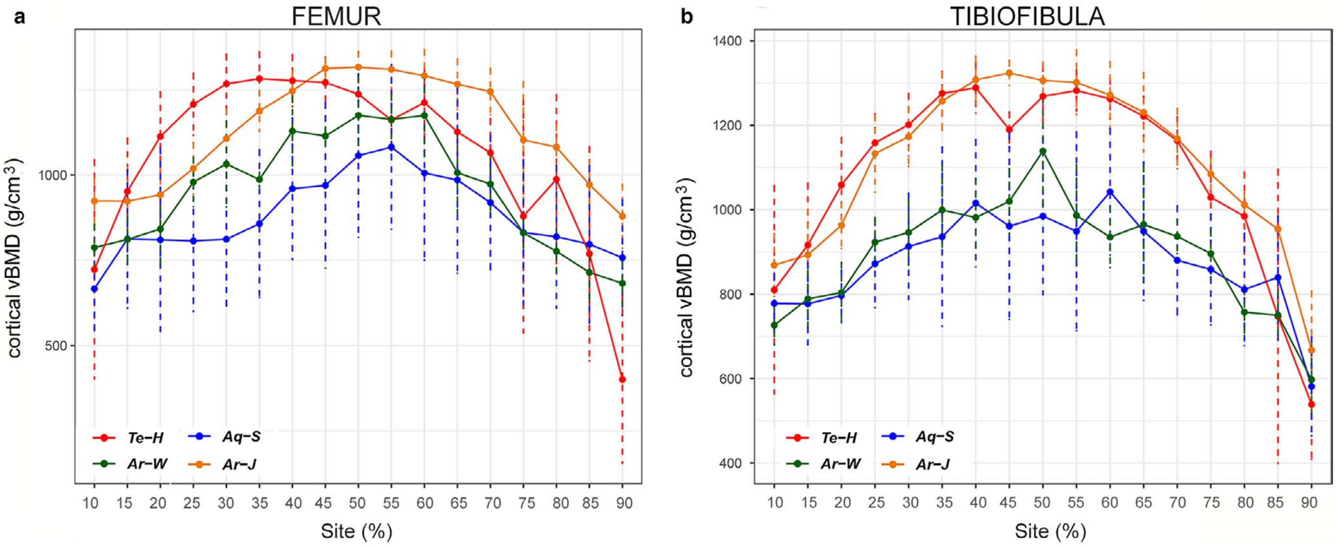

FIGURE 3 Indicator of tissue quality: cortical volumetric bone mineral density (vBMD) of the femur (a), and the tibiofibula (b). Aq-S, aquatic swimmers; Ar-J, arboreal jumpers; Ar-W, arboreal walkers; Te-H, terrestrial-hoppers.

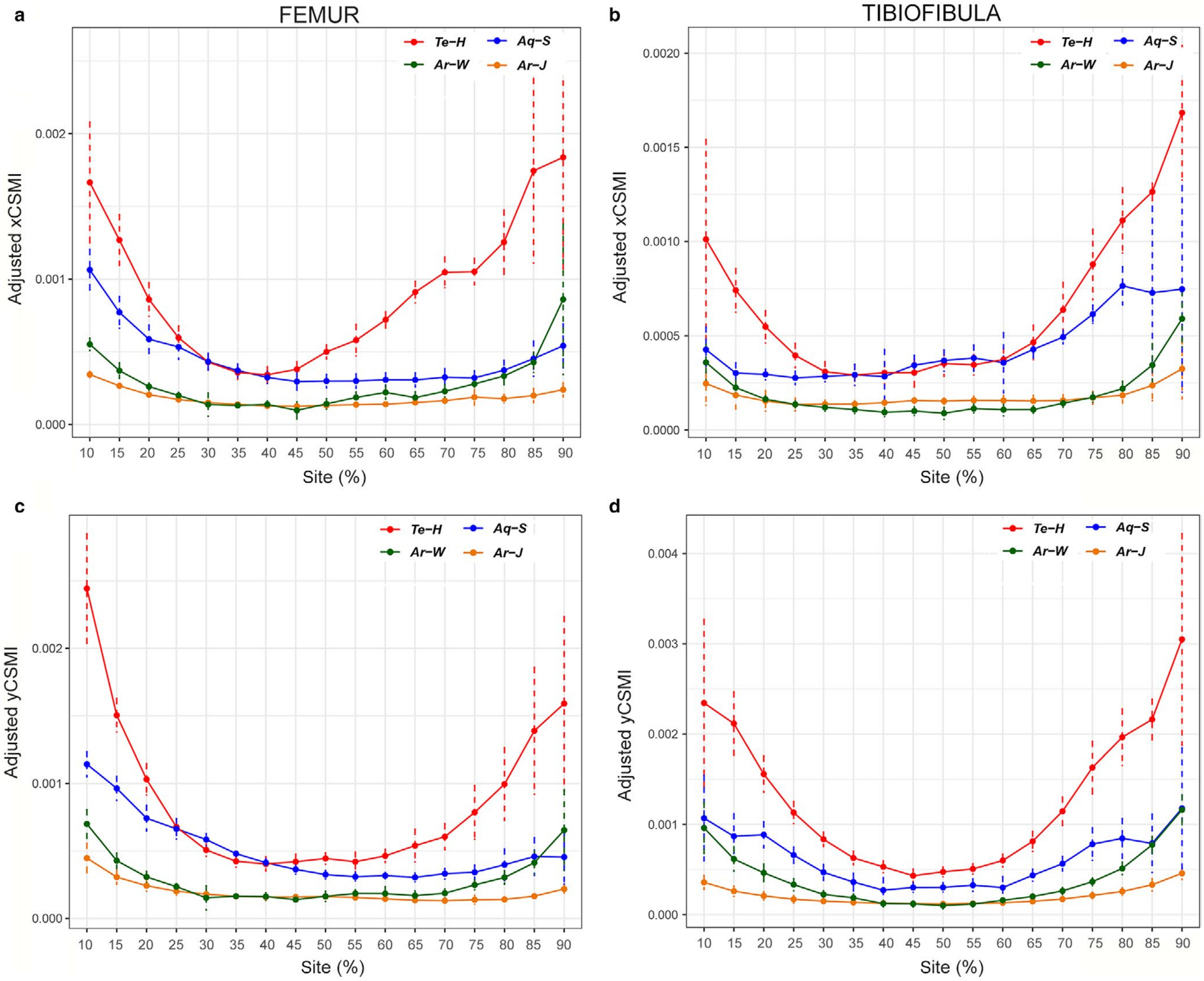

FIGURE 4 Bone design indicators: moment of inertia in *x* and *y* (*x*CSMI, *y*CSMI) of the femur (a,c) and the tibiofibula (b,d). Aq-S, aquatic swimmers; Ar-J, arboreal jumpers; Ar-W, arboreal walkers; Te-H, terrestrial-hoppers.

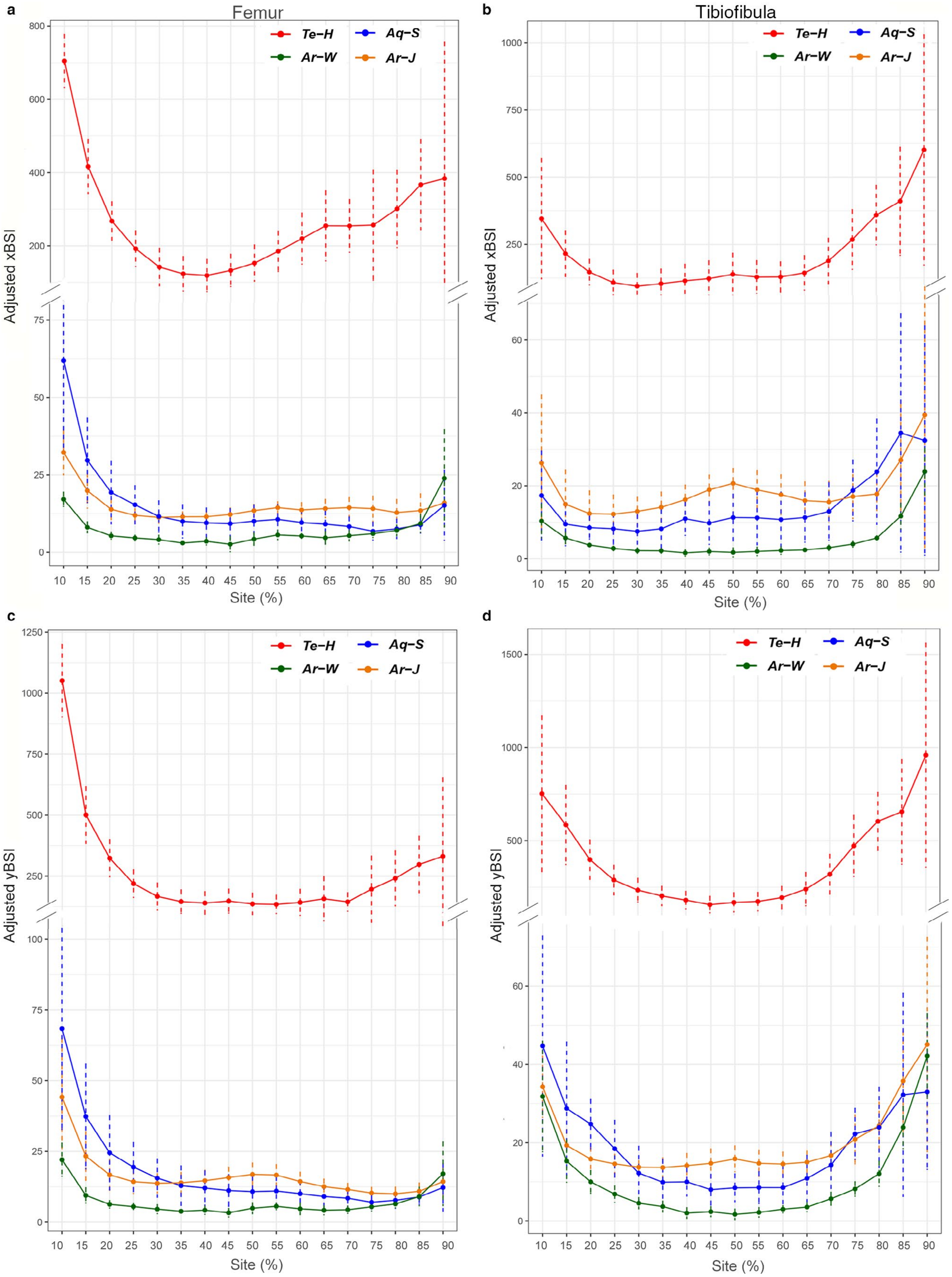

FIGURE 5 Indicators of bone structural strength: bone strength indices in *x* and *y* (*x*BSI, *y*BSI) of the femur (a,c) and the tibiofibula (b,d). Aq-S, aquatic swimmers; Ar-J, arboreal jumpers; Ar-W, arboreal walkers; Te-H, terrestrial-hoppers.

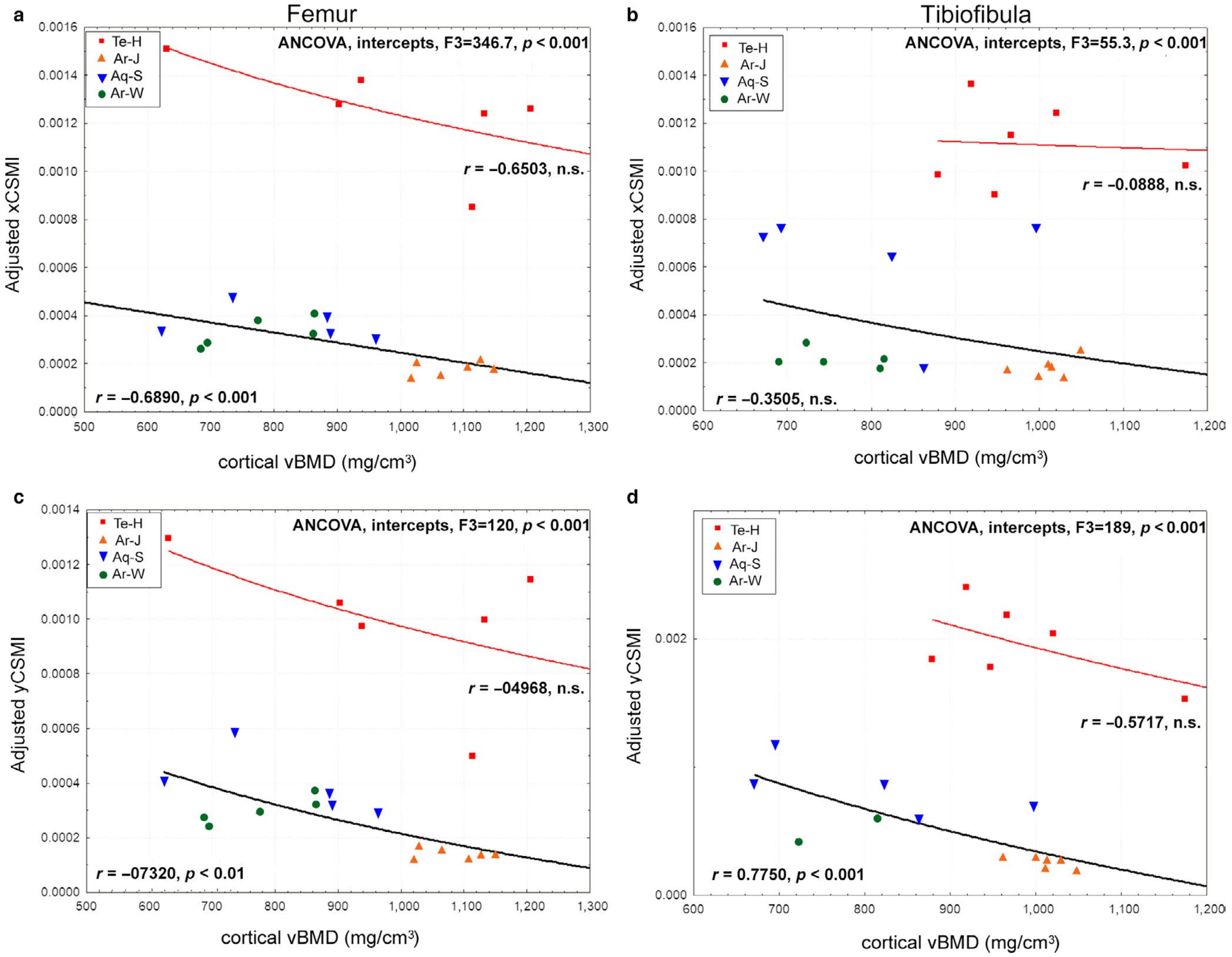

FIGURE 6 Distribution/quality (d/q) curves of the femur (a,c) and the tibiofibula (b,d) at site 80%. Aq-S, aquatic swimmers; Ar-J, arboreal jumpers; Ar-W, arboreal walkers; n.s. not statistical significant;Te-H, terrestrial-hoppers; vBMD, volumetric bone mineral density; *x*CSMI, *y*CSMI, moment of inertia in *x* and *y* in anterior-posterior and lateral bending, respectively.

larger values at the central region than at the bone ends. Higher values for this variable in hopper and jumper species than in walkers and swimmers may reflect an increment of bone formation caused by a more demanding mode of locomotion, as observed in mice subject to physical exercise (Hamrick et al. 2006) and in humans who are trained in different sports (Weidauer et al. 2014; Agostinete et al. 2017a). Aq-S frogs (*Ps. platensis*), the smallest species analyzed, tend to present intermediate values for some allometric variables. Notably, Ar-W species, which are larger than Aq-S species, showed the lowest values for these bone indicators. Thus, the patterns observed in the present study could be explained by the action of external forces (i.e. environment and locomotor modes) that would orient the biomechanical control of the bone resorption/deposition, as stated by Van Der Meulen and Carter (1995) for mammal's species.

Cortical vBMD, strikingly higher at the mid-diaphysis than at the bone ends, as observed in humans (Cointry et al. 2016), was quite similar for the two jumping species (Te-H and Ar-J) and higher in these species than in Aq-S and Ar-W species. Interestingly, Te-H species had the lowest cortical vBMD values at s90 in both bones, as was to be expected because of their lower cortical BMC and higher CtA. As expected, cortical vBMD in aquatic species was found to be the lowest in the study, in congruence with the requirements of life in an aquatic environment. Similar results were reported for human swimmers (Bellew and Gehrig, 2006; Mudd et al. 2007; Agostinete et al. 2017a; Agostinete et al. 2017b) and in rat studies (Bourrin et al. 1992).

An important outcome of our work concerns the differences in loading environments between jumper/hopper and swimmer anurans. It is generally accepted that swimming and jumping imply similar movements produced by the same morphological structures in all frog species (Nauwelaerts et al. 2007; Soliz et al. 2017) since both locomotor modes need the hindlimbs to generate the propulsive forces required (Gillis and Biewener, 2000). Limb movements in an aquatic medium are more strenuous than in an aerial one because of the physical properties of water (Nauwelaerts et al. 2005). Despite this, strain magnitudes in an aquatic environment are much lower than on land (Young and Blob, 2015; Young et al. 2017) because the lack of gravity force and buoyancy reduces the loads placed on the bones supporting the body (Zug, 1971). From our results we can infer that locomotion in an aerial medium is more defiant, as our terrestrial frogs tended to have the best values for all variables. This is in line with reports from Lutz and Rome (1994) and Calow and Alexander (1973), who found that jumping and hopping were more mechanically demanding than swimming. They also observed that the thrust produced during hopping was three to four times greater than during swimming in a small grass frog. In this context, 'normal' gravity would be an essential cofactor for the osteogenic effects of movement (Bourrin et al. 1992), particularly influencing bone remodeling and geometric traits (Demes and Carlson, 2009), which could be enhanced during strong skeletal-loading sessions (Turner and Robling, 2003), as is the case in jumping and hopping.

In the femur and tibiofibula, the adjusted CSMIs showed higher values in both metaphyses, with cortical diameters and area being higher, and lower values in the mid-diaphyses. However, in Te-H species, the adjusted *x*CSMI was significantly larger between S60 and S80 than in the other species, especially in the femurs. This is visibly related to the muscle-insertion crest present at the posterior aspect of the femur section, which is associated with the locomotion mode and the impact generated by the hardness of the ground, which would be similar to that induced by sports such as basketball (Weidauer et al. 2014; Agostinete et al. 2017a). Hopper toads frequently perform several hops in series (Rand, 1952; Zug, 1978; Emerson, 1979), which are often erratic and discontinuous. Hence, their long bones should respond to intense cyclic stress. Large forces and mechanical power are generated rapidly because hopping strides are faster compared with most of the other terrestrial gaits (Emerson, 1985; Lutz and Rome, 1994; Marsh, 1994).

Additionally, the unique kinematics of frog jumping, which requires hindlimb unfolding from a highly crouched position to a straightened position (Calow and Alexander, 1973; Marsh, 1994; Gillis and Biewener, 2000; Kargo and Rome, 2002; Kargo et al. 2002), also subjects frog hindlimb bones to twisting (Blob and Biewener, 1999, 2001; Butcher and Blob, 2008; Butcher et al. 2008) and requires a high bone bending strength. The stiffness of the most distal part of the femur (as assessed by BSI values, especially concerning the *y*-related indicators) reflected a higher resistance to lateral bending, which may reduce the risk of fracture by this type of deformation, a feature that could be highly selective (Cointry et al. 2016). Aq-S species showed intermediate values of both *x*CSMI and *y*CSMI, probably to compensate its lower cortical bone density in a feedback mechanism that controls bone modeling as a function of bone tissue mechanical quality (Ferretti et al. 1993).

Interestingly, in the femur of the arboreal frogs *B. faber*, a jumper species, the CSMIs showed the lowest values, comparable to those found in *P. sauvagii*, a walker species, at s35–s65 sites. Surprisingly, *P. sauvagii* showed high CSMIs values at s70–s90, probably due to the femoral crest. The arboreal frogs studied here move across little branches, i.e. a moving substrate. When little branches move, a balance problem is generated because of the misalignment of the ground reaction force and the frog's center of mass, inducing a rotational moment (Astley et al. 2015). This trend to lower both bone mass indicators (in walker species) and architectural design (in jumper and walker species) in arboreal frogs compared to the other species probably contributes to generating a compensatory behaviour, such as the walker frog's grasping abilities (Manzano et al. 2008; Sustaita et al. 2013; Manzano et al. 2018) and their high ability to adjust their limb posture (Reynaga et al. 2018). Moreover, the general movements of these frogs are slow, decreasing the chances of falling from the branches, which would be highly risky for bones of such poor quality.

The bone structural indicators (BSIs) were always higher in Te-H species, while the Aq-S and Ar-J species had intermediate values, and Ar-W species had comparatively low values. A higher structural bone stiffness/strength is associated with strong musculature (Frost et al. 1998; Schoenau, 2005) and concomitantly higher mechanical loads (Turner and Robling, 2003) such as those supported by bones of terrestrial species. This feature is consistent with considerable resistance to fracture (Leung et al. 2003). By contrast, the Ar-W species, such as *P. sauvagii*, have more flexible bones. In fact, bone deformation allows for elastic energy storage that can optimize locomotion biomechanics. Moreover, hindlimb bone strength is not only influenced by the musculature and mechanical loads, but also by the mobility of the ankle experienced by the limb in arboreal and terrestrial environments (Marchi, 2015). Taken together, the differences observed in the present study between the two arboreal species can also be attributed to ankle mobility since they have very different limb postures.

The observed d/q relationships support our second hypothesis. They were always described by negative, hyperbolically shaped functions, as usually observed when comparing any pair of variables which are mutually inter-related by a feedback control system (Ferretti, 1995; Ferretti et al. 1995; Di Masso et al. 1997; Feldman et al. 2004; Cointry et al. 2005, 2013, 2016). With the exception of Te-H species (*R. diptycha*), the curves for the species studied showed a common significant negative trend, regardless of the mode of locomotion or the habitat (Figure 6a–d). The species that had a lower density (Aq-S and Ar-W) would appear to compensate for it by achieving a better cross-sectional design (CSMIs) at s70–s90, compared with the Ar-J species. By contrast, values for *R. diptycha* were plotted at the upper zone of the graph, with a significant difference in ordinates compared with the other curves. This result could indicate that the adaptation of *R. diptycha* bones to a terrestrial environment and mode of locomotion (hopping) would involve the development of larger CSMIs regardless of the tissue compliance to be deformed, suggesting the interaction of some morphogenetic factors in the determination of long-bone architectural design.

In conclusion, our findings support both hypotheses and we conclude the following:

1. The femur and tibiofibula measures showed differences among the different species analyzed, especially in the Te-H species:
    - Cortical vBMD was strikingly higher in jumpers (*B. faber*) and hoppers (*R. diptycha*) than in other species, regardless of the environment. Clearly, swimmers (*Ps. platensis*) and Ar-W species (*P. sauvagii*) had lower cortical bone density.
    - As expected, the larger size of *R. diptycha* significantly influenced the allometric and structural indicators. Moreover, *P. sauvagii*, an intermediate-sized species, and *Ps. platensis*, the smallest species, had the lowest and intermediates values of these indicators, respectively, suggesting a similar mechanical influence.
    - Bone design indicators showed quite similar trends in all species, although they were higher in *R. diptycha* than in the other species. Strikingly, both moments of inertia had intermediate values in *Ps. platensis* and lower values in *B. faber* and *P. sauvagii*. This would mean that both locomotor mode and terrestrial environment should stimulate the development of a high xCSMI. It seems as if *Ps. platensis* (Aq-S) would have better compensated for its lower cortical bone density.
    - The bone structural indicators, in general, were higher in *R. dypticha* and *Ps. platensis*, while *B. faber* had intermediate values, and *P. sauvagii* had comparatively low values. These findings could indicate that arboreal species would have greater flexibility than terrestrial and aquatic species owing to their slow displacements on the branches, especially in the walking species *P. sauvagii*, which is subject to less impact than the jumper *B. faber*.
2. The d/q relationships observed for aquatic and arboreal species suggest that the bone mechanostat responds to mechanical demands, compensating for low bone densities by improving bone design, as we have observed in other studies. However, the size-shape adjusted data of *R. diptycha* plotted distinctly, in the 'anabolic' zone of the graph, compared with those who were adjusted to the other curve. This would indicate that the allometric differences between bones of this and the other species should also be determined significantly by some mechanically unrelated, morphogenetic factors.

Our study may represent one of the first attempts to analyze the geometrical and structural properties of the bones in anurans within a morpho-functional comparative context. It should be considered, however, that we have disregarded the phylogenetic signal of our data since the sample was too small. Despite this, differences in bone properties within the same clade, as recorded in hylids, suggest that the mechanical environment where the species develop can drive a considerable proportion of their skeletal traits.

ACKNOWLEDGEMENTS

We thank Dr Diego Baldo, curator of the herpetological collection of the *Laboratorio de Genetica Evolutiva* of *Instituto de Biologia Subtropical*, for providing the study material. We are very grateful to Dr Ricardo F. Capozza for his technical help with pQCT and osteology concepts and to two anonymous reviewers who made relevant suggestions to enhance the manuscript. This research received support from PIP 0389 and PICT 2016-2772 to VA. M.C.V. was supported by CONICET Postdoctoral Fellowship.

CONFLICTS OF INTEREST

None declared.

DATA AVAILABILITY STATEMENT

The data that support the findings of this study are available from the corresponding author upon reasonable request.

ORCID

Miriam Corina Vera https://orcid.org/0000-0003-0988-1345
Virginia Abdala https://orcid.org/0000-0002-4615-5011

REFERENCES

Agostinete, R.R., Duarte, J.P., Valente-Dos-Santos, J., et al. (2017a) Bone tissue, blood lipids and inflammatory profiles in adolescent male athletes from sports contrasting in mechanical load. *PLoS ONE*, 12(6), e0180357.

Agostinete, R.R., Maillane-Vanegas, S., Lynch, K.R., et al. (2017b) The impact of training load on bone mineral density of adolescent swimmers: a structural equation modeling approach. *Pediatric Exercise Science*, 29(4), 520–528. https://doi.org/10.1123/pes.2017-0008

Astley, H.C., Haruta, A. and Roberts, T.J. (2015) Robust jumping performance and elastic energy recovery from compliant perches in tree frogs. *Journal of Experimental Biology*, 218, 3360–3363. https://doi.org/10.1242/jeb.121715

Bauwens, D., Garland Jr, T., Castilla, A.M., et al. (1995) Evolution of sprint speed in lacertid lizards: morphological, physiological and behavioral covariation. *Evolution*, 49, 848–863.

Bellew, J.W. and Gehrig, L. (2006) A comparison of bone mineral density in adolescent female swimmers, soccer players, and weight lifters. *Pediatric Physical Therapy*, 18, 19–22.

Biewener, A.A. and Gillis, G.B. (1999) Dynamics of muscle function during locomotion: accommodating variable conditions. *Journal of Experimental Biology*, 23, 3387–3396.

Bourrin, S., Ghaemmaghami, F., Vico, L., et al. (1992) Effect of a five-week swimming program on rat bone: a histomorphometric study. *Calcified Tissue International*, 51, 137–142.

Blob, R.W. and Biewener, A.A. (1999) In vivo locomotor strain in the hindlimb bones of *Alligator mississippiensis* and Iguana iguana: implications for the evolution of limb bone safety factor and non-sprawling limb posture. *Journal of Experimental Biology*, 202, 1023–1046.

Blob, R.W. and Biewener, A.A. (2001) Mechanics of limb bone loading during terrestrial locomotion in the green iguana (*Iguana iguana*) and american alligator (*Alligator mississippiensis*). *Journal of Experimental Biology*, 204, 1099–1122.

Blob, R.W. and Snelgrove, J.M. (2006) Antler stiffness in moose (*alces alces*): correlated evolution of bone function and material properties? *Journal of Morphology*, 1086, 1075–1086.

Broshko, Y.O. (2014) Variability of structural and biomechanical parameters of pelophylax esculentus (Amphibia, Anura) limb bones. *Vestnik Zoologii*, 48, 239–248.

Butcher, M.T. and Blob, R.W. (2008) Mechanics of limb bone loading during terrestrial locomotion in river cooter turtles (Pseudemys concinna). *Journal of Experimental Biology*, 211, 1187–1202.

Butcher, M.T., Espinoza, N.R., Cirilo, S.R., et al. (2008) In vivo strains in the femur of river cooter turtles (Pseudemys concinna) during terrestrial locomotion: tests of force-platform models of loading mechanics. *Journal of Experimental Biology*, 211, 2397–2407.

Calow, L.J. and Alexander, R.M. (1973) A mechanical analysis of a hind leg of a frog (Rana temporaria). *Journal of Zoology*, 171, 293–321.

Carter, D.R., Mikic, B. and Padian, K. (1998) Epigenetic mechanical factors in the evolution of long bone epiphyses. *Zoological Journal of the Linnean Society*, 123, 163–178.

Cointry, G.R., Capozza, R.F., Chiappe, M.A., et al. (2005) Novel experimental effects on bone material properties and the pre-and post-yield behavior of bones may be independent of bone mineralization. *Journal of Bone and Mineral Metabolism*, 23, 30–35.

Cointry, G.R., Reina, P., Nocciolino, L., et al. (2013) Z-scoring of pQCT-assessed, reference distribution/quality curves in the human tibia to evaluate the efficiency of bone mechanostat. *Bone*, 53(2), 604. https://doi.org/10.1016/j.bone.2012.12.040

Cointry, G.R., Ferretti, J.L., Reina, P.S., et al. (2014) The pQCT “Bone Strength Indices”(BSIs, SSI). Relative mechanical impact and diagnostic value of the indicators of bone tissue and design quality employed in their calculation in healthy men and pre-and post-menopausal women. *Journal of Musculoskeletal and Neuronal Interactions*, 14, 29–40.

Cointry, G.R., Nocciolino, L., Ireland, A., et al. (2016) Structural differences in cortical shell properties between upper and lower human fibula as described by pQCT serial scans. A biomechanical interpretation. *Bone*, 90, 185–194.

Cox, S. and Gillis, G. (2015) Forelimb kinematics during hopping and landing in toads (*Bufo marinus*). *Journal of Experimental Biology*, 218, 3051–3058.

Currey, J.D. (1999) What determines the bending strength of com- pact bone? *Journal of Experimental Biology*, 202, 2495–2503.

Cruz, F.B., Belver, L., Acosta, J.C., et al. (2009) Thermal biology of phymaturus lizards: evolutionary constraints or lack of environmental variation? *Zoology*, 112, 425–432.

Demes, B. and Carlson, K.J. (2009) Locomotor variation and bending regimes of capuchin limb bones. *American Journal of Physical Anthropology*, 139, 558–571.

Di Masso, R.J., Font, M.T., Capozza, R.F., et al. (1997) Long-bone biomechanics in mice selected for body conformation. *Bone*, 20, 539–545.

Duellman, W. and Trueb, L. (1986) *Biology of Amphibians*. New York, NY: McGraw-Hill.

Emerson, S.B. (1979) The ilio-sacral articulation in frogs: Form and function. *Biological Journal of the Linnean Society*, 11, 153–168.

Emerson, S.B. (1985) Jumping and leaping. In: Hildebrand, M., Bramble, D.M., Leim, K.F. and Wake, D.B. (Eds.) *Functional Vertebrate Anatomy*. Cambridge, MA: Belknap Press, pp. 58–72.

Feldman, S., Cointry, G.R., Duarte, M.E.L., et al. (2004) Effects of hypophysectomy and recombinant human growth hormone on material and geometric properties and the pre-and post-yield behavior of femurs in young rats. *Bone*, 34, 203–215.

Feldman, S., Capozza, R.F., Mortarino, P.A., et al. (2012) Site and sex effects on tibia structure in distance runners and untrained people. *Medicine and Science in Sports and Exercise*, 44, 1580–1588.

Ferretti, J.L. (1995) Perspectives of pQCT technology associated to biomechanical studies in skeletal research employing rat models. *Bone*, 17, 353–364.

Ferretti, J.L. (1998) Biomechanical properties of bone. In: Genant, H.K., Guglielmi, G. and Jergas, M. (Eds.) *Bone Densitometry and Osteoporosis*. Berlin, Germany: Springer, pp. 143–161.

Ferretti, J.L., Capozza, R.F., Mondel, N., et al. (1993) Interrelationships between densitometric, geometric, and mechanical properties of rat femora: Inferences concerning mechanical regulation of bone modeling. *Journal of Bone and Mineral Research*, 8, 1389–1396.

Ferretti, J.L., Frost, H.M., Gasser, J.A., et al. (1995) Perspectives on osteoporosis research: its focus and some insights from a new paradigm. *Calcified Tissue International*, 57, 399–404. https://doi.org/10.1007/BF00301939

Ferretti, J.L., Capozza, R.F. and Zanchetta, J.R. (1996) Mechanical validation of a tomographic (pQCT) index for noninvasive estimation of rat femur bending strength. *Bone*, 18, 97–102. https://doi.org/10.1016/8756-3282(95)00438-6

Ferretti, J.L., Cointry, G.R., Capozza, R.F., et al. (2001) Analysis of biomechanical effects on bone and on the muscle-bone interactions in small animal models. *Journal of Musculoskeletal & Neuronal Interactions*, 1, 263–274.

Fratani, J., Ponssa, M.L. and Abdala, V. (2018) Evolution of tendon shape in an anuran clade and its relation to size, phylogeny and locomotion. *Journal of Zoology*, 307, 233–241.

Frost, H.M. (1990) Skeletal structural adaptations to mechanical usage (SATMU): 1. Redefining Wolff’s law: The bone modeling problem. *Anatomical Record*, 226, 403–413.

Frost, H.M. (1998) Changing concepts in skeletal physiology: Wolff's Law, the mechanostat, and the “Utah Paradigm”. *American Journal of Human Biology*, 10(5), 599–605. https://doi.org/10.1002/(SICI)1520-6300(1998)10:5<599:AID-AJHB6>3.0.CO;2-9

Frost, H.M. (2002) *The Utah Paradigm of Skeletal Physiology* (Ed.). Ismini, Athens.

Frost, H.M., Ferretti, J.L. and Jee, W.S.S. (1998) Perspectives: some roles of mechanical usage, muscle strength, and the mechanostat in skeletal physiology, disease, and research. *Calcified Tissue International*, 62, 1–7. https://doi.org/10.1007/s002239900384

Gomez-Bruton, A., Montero-Marín, J., González-Aguero, A., et al. (2015) The effect of swimming during childhood and adolescence on bone mineral density: a systematic review and meta-analysis. *Sports Medicine*, 46(3), 365–379. https://doi.org/10.1007/s40279-015-0427-3

Gillis, G.B. and Biewener, A.A. (2000) Hindlimb extensor muscle function during jumping and swimming in the toad (*Bufo marinus*). *Journal of Experimental Biology*, 203, 3547–3563.

Guilluy, C., Osborne, L.D., Van Landenghem, L., et al. (2014) Isolated nuclei adapt to force and reveal a mechanotransduction pathway in the nucleus. *Nature Cell Biology*, 16(4), 376–381. https://doi.org/10.1038/ncb2927

Griep, S., Schilling, N., Marshall, P., et al. (2013) Pectoral girdle movements and the role of the glenohumeral joint during landing in the toad, *Rhinella marina* (Linnaeus, 1758). *Zoomorph*, 132, 325–338. https://doi.org/10.1007/s00435-013-0189-0

Hamrick, M.W., Skedros, J.G., Pennington, C., et al. (2006) Increased osteogenic response to exercise in metaphyseal versus diaphyseal cortical bone. *Journal of Musculoskeletal and Neuronal Interactions*, 6, 258–263.

Herrel, A., Vasilopoulou-Kampitsi, M., and Bonneaud, C. (2014) *Jumping Performance in the Highly Aquatic Frog, Xenopus tropicalis: Sex-Specific Relationships Between Morphology and Performance*. – PeerJ 2: e66.

Hudson, N.J., Bennett, M.B. and Franklin, C.E. (2004) Effect of aestivation on long bone mechanical properties in the green-striped burrowing frog, *Cyclorana alboguttata. Journal of Experimental Biology*, 207, 475–482.

Humphries, D.L., Grogan, J.A. and Gaffney, E.A. (2017) Mechanical cell-cell communication in fibrous networks: the importance of network geometry. *Bulletin of Mathematical Biology*, 79, 498–524. https://doi.org/10.1007/s11538-016-0242-5

Iskratsch, T., Wolfenson, H. and Sheetz, M.P. (2014) Appreciating force and shape - the rise of mechanotransduction in cell biology. *Nature Reviews Molecular Cell Biology*, 15, 825–833.

Kargo, W.J. and Rome, L.C. (2002) Functional morphology of proximal hindlimb muscles in the frog *Rana pipiens*. *Journal of Experimental Biology*, 205, 1987–2004.

Kargo, W.J., Nelson, F. and Rome, L.C. (2002) Jumping in frogs: assessing the design of the skeletal system by anatomically realistic modeling and forward dynamic simulation. *Journal of Experimental Biology*, 205, 1683–1702.

Kontulainen, S.A., Johnston, J.D., Liu, D., et al. (2008) Strength indices from pQCT imaging predict up to 85 % of variance in bone failure properties at tibial epiphysis and diaphysis. *Journal of Musculoskeletal and Neuronal Interactions*, 8, 401–409.

Leung, K.S., Siu, W.S. and Qin, L. (2003) pQCT bone strength index may serve as a better predictor than bone mineral density for long bone breaking strength. *Journal of Bone and Mineral Metabolism*, 21, 316–322.

Losos, J.B. (1990a) Ecomorphology, performance capability and scaling of West Indian Anolis lizards: an evolutionary analysis. *Ecological Monographs*, 60, 369–388. https://doi.org/10.2307/1943062

Losos, J.B. (1990b) Concordant evolution of locomotor behaviour, display rate and morphology in Anolis lizards. *Animal Behavior*, 39, 879–890. https://doi.org/10.1016/S0003-3472(05)80952-2

Losos, J.B. (1990c) The evolution of form and function: Morphology and locomotor performance in indian Anolis lizards. *Evolution*, 44, 1189–1203.

Losos, J.B., Andrews, R.M., Sexton, O.J., et al. (1991) Behavior, ecology, and locomotor performance of the giant Anole. Anolis frenatus. *Caribbean Journal of Science*, 27, 173–179.

Lutz, G.J. and Rome, L.C. (1994) Built for jumping: the design of the frog muscular system. *Science*, 263, 370–372.

Manzano, A.S., Abdala, V. and Herrel, A. (2008) Morphology and function of the forelimb in arboreal frogs: specializations for grasping ability? *Journal of Anatomy*, 213, 296–307. https://doi.org/10.1111/j.1469-7580.2008.00929.x

Manzano, A.S., Herrel, A., Fabre, A., et al. (2017) Variation in brain anatomy in frogs and its possible bearing on their locomotor ecology. *Journal of Anatomy*, 231, 38–58.

Manzano, A.S., Fontanarrosa, G. and Abdala, V. (2018) Manual and pedal grasping among anurans: a review of relevant concepts with empirical approaches. *Biological Journal of the Linnean Society*, 127, 598–610.

Marchi, D. (2015) Variation in tibia and fibula diaphyseal strength and its relationship with arboreal and terrestrial locomotion: extending the investigation to non-hominoid primates. *Journal of Anthropological Sciences*, 93, 153–156.

Marsh, R.L. (1994) Jumping ability of anuran amphibians. *Advances in Veterinary Science and Comparative Medicine*, 38, 51–111.

Morseth, B., Emaus, N. and Jørgensen, L. (2011) Physical activity and bone: the importance of the various mechanical stimuli for bone mineral density. A review. *Norsk Epidemiologi*, 20(2), 173–178. https://doi.org/10.5324/nje.v20i2.1338

Mudd, L.M., Fornetti, W. and Pivarnik, J.M. (2007) Bone mineral density in collegiate female athletes: comparisons among sports. *Journal of Athletic Training*, 42, 403–408.

Nadell, J.A. and Shaw, C.N. (2015) Phenotypic plasticity and constraint along the upper and lower limb diaphyses in Homo sapiens. *American Journal of Physical Anthropology*, 159, 410–422.

Nauwelaerts, S. and Aerts, P. (2003) Propulsive impulse as a covarying performance measure in the comparison of the kinematics of swimming and jumping in frogs. *Journal of Experimental Biology*, 206, 4341–4351.

Nauwelaerts, S., Stamhuis, E. and Aerts, P. (2005) Swimming and jumping in a semi-aquatic frog. *Animal Biology*, 55(1), 3–15. https://doi.org/10.1163/1570756053276934

Nauwelaerts, S., Ramsay, J. and Aerts, P. (2007) Morphological correlates of aquatic and terrestrial locomotion in a semi-aquatic frog, *Rana esculenta*: no evidence for a design conflict. *Journal of Anatomy*, 210, 304–317.

Rand, S.A. (1952) Jumping ability of certain anurans, with notes on endurance. *Copeia*, 1952, 15–20. https://doi.org/10.2307/1437615

Reynaga, C.M., Astley, H.C. and Azizi, E. (2018) Morphological and kinematic specializations of walking frogs. *Journal of Experimental Zoology Part A: Ecological and Integrative Physiology*, 329(2), 87–98. https://doi.org/10.1002/jez.2182

Reynaga, C.M., Caitrin, E., Strong, G., et al. (2019) Compliant substrates disrupt elastic energy storage in jumping tree frogs. *Integrative and Comparative Biology*, 59(6), 1535–1545. https://doi.org/10.1093/icb/icz069

Rittweger, J., Michaeli, I., Giehl, M., et al. (2004) Adjusting for the partial volume effect in cortical bone analyses of pQCT images. *Journal of Musculoskeletal and Neuronal Interactions*, 4, 436–441.

Rolfe, R.A., Nowlan, N.C., Kenny, E.M., et al. (2014) Identification of mechanosensitive genes during skeletal development: alteration of genes associated with cytoskeletal rearrangement and cell signaling pathways. *Genomics*, 15, 48–56.

Ruff, C.B. (2000) Body size, body shape, and long bone strength in modern humans. *Journal of Human Evolution*, 38, 269–290. https://doi.org/10.1006/jhev.1999.0322

Sustaita, D., Pouydebat, E., Manzano, A., et al. (2013) Getting a grip on tetrapod grasping: form, function, and evolution. *Biological Reviews*, 88, 380–405. https://doi.org/10.1111/brv.12010

Schoenau, E. (2005) From mechanostat theory to development of the "Functional Muscle-Bone-Unit". *Journal of Musculoskeletal and Neuronal Interactions*, 5, 232–238.

Tulli, M.J., Abdala, V. and Cruz, F.B. (2011) Relationships among morphology, clinging performance and habitat use in Liolaemini lizards. *Journal of Evolutionary Biology*, 24, 843–855. https://doi.org/10.1111/j.1420-9101.2010.02218.x

Turner, C.H. and Robling, A.G. (2003) Designing exercise regimens to increase bone strength. *Exercise and Sport Sciences Reviews*, 31, 45–50. https://doi.org/10.1097/00003677-200301000-00009

Tondon, A. and Kaunas, R. (2014) The direction of stretch-induced cell and stress fiber orientation depends on collagen matrix stress. *PLoS ONE*, 9, e89592. https://doi.org/10.1371/journal.pone.0089592

Soliz, M., Tulli, M.J. and Abdala, V. (2017) Osteological postcranial traits in hylid anurans indicate a morphological continuum between swimming and jumping locomotor modes. *Journal of Morphology*, 278, 403–417. https://doi.org/10.1002/jmor.20651

Van Der Meulen, M.C. and Carter, D.R. (1995) Developmental mechanics determine long bone allometry. *Journal of Theoretical Biology*, 172, 323–327. https://doi.org/10.1006/jtbi.1995.0029

Vera, M.C., Abdala, V., Aráoz, E., et al. (2018) Movement and joints: effects of overuse on anuran knee tissues. *PeerJ*, 6, e5546. https://doi.org/10.7717/peerj.5546

Vizcaíno, S.F., Bargo, M.S., Cassini, G.H., et al. (2016) Preferencia y uso del sustrato. Locomoción en el medio terrestre. In: Vizcaíno, S.F., Bargo, M.S., Cassini, G.H., and Toledo, N. (Eds). *Forma Y Función En Paleobiología De Vertebrados*. La Plata, Buenos Aires: Editorial de la Universidad Nacional de La Plata (EDULP), pp. 118–135.

Wang, N., Tytell, J.D. and Ingber, D.E. (2009) Mechanotransduction at a distance: mechanically coupling the extracellular matrix with the nucleus. *Nature Reviews*, 10, 75–85. https://doi.org/10.1038/nrm2594

Weidauer, L., Minett, M., Negus, C., et al. (2014) Odd - impact loading results in increased cortical area and moments of inertia in collegiate athletes. *European Journal of Applied Physiology*, 114, 1429–1438. https://doi.org/10.1007/s00421-014-2870-5

Wilson, M.P., Espinoza, N.R., Shah, S.R., et al. (2009) Mechanical properties of the hindlimb bones of bullfrogs and cane toads in bending and torsion. *The Anatomical Record*, 292, 935–944. https://doi.org/10.1002/ar.20929

Young, V.K.H. and Blob, R.W. (2015) Limb bone loading in swimming turtles: changes in loading facilitate transitions from tubular to flipper-shaped limbs during aquatic invasions. *Biology Letters*, 11, 20150110. https://doi.org/10.1098/rsbl.2015.0110

Young, V.K.H., Wienands, C.E., Wilburn, B.P., et al. (2017) Humeral loads during swimming and walking in turtles: implications for morphological change during aquatic reinvasions. *Journal of Experimental Biology*, 220, 3873–3877. https://doi.org/10.1242/jeb.156836

Zug, G.R. (1971) *Buoyancy, Locomotion, Morphology of the Pelvic Girdle and Hind Limb, and Systematics of Cryptodiran Turtles*. Misc. Publ. Mus. Zool. Univ. Mich., 142, 1–98.

Zug, G.R. (1978) *Anuran Locomotion -Structure and Function, 2: Jumping Performance of Semiaquatic, Terrestrial, and Arboreal Frogs (No. 276)*. Washington, DC: Smithsonian Institution Press.

How to cite this article: Vera MC, Ferretti JL, Abdala V, Cointry GR. Biomechanical properties of anuran long bones: correlations with locomotor modes and habitat use. *J. Anat.*. 2020;00:1–14. https://doi.org/10.1111/joa.13161